

June 2008

Microfluidic electroporation for delivery of small molecules and genes into cells using a common DC power supply

Hsiang-Yu Wang

Purdue University, hwang@purdue.edu

Chang Lu

Birck Nanotechnology Center, Purdue University, changlu@purdue.edu

Follow this and additional works at: <http://docs.lib.purdue.edu/nanopub>

Wang, Hsiang-Yu and Lu, Chang, "Microfluidic electroporation for delivery of small molecules and genes into cells using a common DC power supply" (2008). *Birck and NCN Publications*. Paper 177.

<http://docs.lib.purdue.edu/nanopub/177>

This document has been made available through Purdue e-Pubs, a service of the Purdue University Libraries. Please contact epubs@purdue.edu for additional information.

Microfluidic Electroporation for Delivery of Small Molecules and Genes Into Cells Using a Common DC Power Supply

Hsiang-Yu Wang,¹ Chang Lu^{1,2,3,4}

¹School of Chemical Engineering, Purdue University, West Lafayette, Indiana; telephone: 765-494-1188; fax: 765-496-1115; e-mail: changlu@purdue.edu

²Department of Agricultural and Biological Engineering, Purdue University, 225 S. University Street, West Lafayette, Indiana 47907

³Birck Nanotechnology Center, Purdue University, West Lafayette, Indiana

⁴Bindley Bioscience Center, Purdue University, West Lafayette, Indiana

Received 8 July 2007; revision received 15 October 2007; accepted 4 December 2007

Published online 8 January 2008 in Wiley InterScience (www.interscience.wiley.com). DOI 10.1002/bit.21784

ABSTRACT: Electroporation is an efficient method of introducing foreign impermeant molecules such as drugs and genes into cells. Conventional electroporation has been based on the application of short electrical pulses (electropulsation). Electropulsation requires specialized equipment and cannot be integrated easily with techniques such as electrophoresis which is based on constant voltage. Here we demonstrate the delivery of small molecules and genes into cells, using a microfluidic electroporation technique based on constant direct current (DC) voltage that we developed earlier. We demonstrate the delivery of two molecules into Chinese hamster ovary (CHO-K1) cells: a membrane impermeable nucleic acid dye (SYTOX[®] Green) and a plasmid vector carrying the gene for green fluorescent protein (pEGFP-C1). Our devices can exert field variations to flowing cells that are analogous to the application of single or multiple pulses by having different geometries. We investigate the effects of the electrical parameters and different geometries of the device on the transfection efficiency and cell viability. Our technique provides a simple solution to electroporation-based drug and gene delivery by eliminating the need for a pulse generator. We envision that these simple microscale electroporation devices will have the potential to work in parallel on a microchip platform and such technology will allow high-throughput functional screening of drugs and genes.

Biotechnol. Bioeng. 2008;100: 579–586.

© 2008 Wiley Periodicals, Inc.

KEYWORDS: electroporation; microfluidics; transfection; gene delivery; drug delivery

Introduction

Since demonstrated for drug and gene delivery in 1980s (Neumann et al., 1982; Okino and Mohri, 1987), electroporation has become an established procedure to deliver impermeant molecules into mammalian cells. The conventional electroporation typically applies short electrical pulses to diminish the excessive heating and damage to cells due to the electric current. A pulse generator such as special capacitor discharge equipment is required to generate the high voltage pulses. Recently a number of microfluidics-based electroporation techniques have been developed. By reducing the distance between microscale electrodes (Lee and Tai, 1999; Lin and Huang, 2001; Lu et al., 2005) or creating physical constraints with subcellular dimensions (Huang and Rubinsky, 2003; Khine et al., 2005; Munce et al., 2004), the voltage applied for electroporation was significantly decreased compared to that in conventional electropulsation. However, in these devices electrical pulses were still applied when cell viability needed to be preserved for gene or drug delivery purposes (Huang and Rubinsky, 2003; Lin and Huang, 2001). The requirement of a pulse generator increased the cost for these devices. More importantly, electricity in pulse form is not compatible with other analytical tools such as electrophoresis which requires constant DC voltage.

In recent work, we have demonstrated that when the cross-sectional area of a microfluidic channel altered in different sections, it was possible to have electroporation occur exclusively in the section with small cross-sectional area but not in the other sections where the cross-sectional area was large (Wang and Lu, 2006; Wang HY et al., 2006). Such variation in the cross-sectional area of the channel can be easily realized by having different widths in various sections when the depth of the channel is uniform. In

Correspondence to: C. Lu

this study, we demonstrate the delivery of impermeant small molecules and plasmid vectors into cells using this microfluidics-based electroporation technique under constant DC voltage provided by a common DC power supply. Devices with different geometries were applied to gene delivery. We report the effects of the device geometry and the electrical parameters on the delivery efficiency in detail.

Materials and Methods

Mathematic Modeling of the Field Intensity in the Microfluidic Device

The Conductive Media DC model from Comsol 3.2 (COMSOL, Inc., Burlington, MA) was applied to model the electric field distribution in Figure 1b. We assumed no ion concentration gradient in the flowing fluid carrying the current and no presence of heating. The continuity equation $\nabla \cdot J = Q$, in which J is the current density and Q is the current source, combined with the definitions of $J = \sigma E$ and $E = -\nabla V$ (E is the electric field and V is the voltage), yields the Poisson's equation. With the absence of the current source, it reduces to Laplace equation:

$$\nabla \cdot (-\sigma \nabla V) = 0$$

where σ is the conductivity (S/m). For our buffer system the conductivity is isotropic and we used 0.127 S/m as the value of σ (Pavlin et al., 2005). We applied the following boundary conditions:

- $n \cdot J = 0$ (electrically insulated) at $Y = \pm 250 \mu\text{m}$ in wide sections and at $Y = \pm 31.25 \mu\text{m}$ in the narrow sections for all configurations,

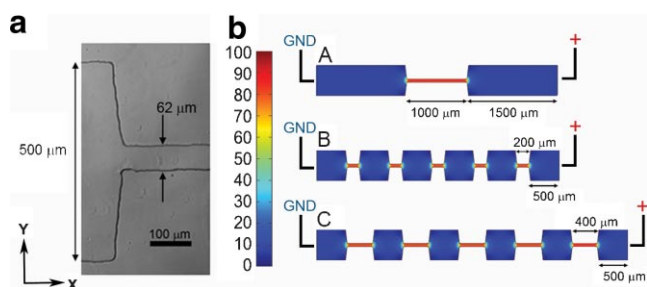


Figure 1. The design of the electroporation devices and the modeling of the field intensity distribution inside the devices. **a:** The optical image showing the width reduction at the junction of the narrow and wide sections. In all devices, the widths of the wide and narrow sections were 500 and 62 μm , respectively. The depth of the channel was around 48 μm . **b:** Mathematical modeling (Comsol 3.2) of the field intensity distribution in devices of different configurations. We assigned 100 to the field intensity at the center of the narrow section. We used three configurations (A, B, and C) in different experiments. The lengths of different sections are labeled in the figure. [Color figure can be seen in the online version of this article, available at www.interscience.wiley.com.]

- $V =$ the applied voltage at $X = 4 \text{ mm}$ for configuration A and B, at $X = 5 \text{ mm}$ for configuration C,
- $V = 0$ at $X = 0$ for all configurations.

The central axis and the left end of the channel were designated as $Y = 0$ and $X = 0$. As an example, the number of elements, the number of boundary elements and the minimum element quality were 62,512, 1,096, and 0.4907 in the simulation of the configuration A device.

Fabrication of the Devices

The device was fabricated using standard soft lithography and the detailed procedure was provided in our previous publication (Wang and Lu, 2006). Briefly, microscale features that served as masters for molding microfluidic channels were made on 3 in. silicon wafers following standard lithography process using negative photoresist (SU-8 2025, MicroChem Corp., Newton, MA). A thick layer ($\sim 5 \text{ mm}$) of polydimethylsiloxane (PDMS, General Electric Silicones RTV 615, MG chemicals, Toronto, Canada) was poured onto the master and then baked for 30 min at 80°C . After baking, the cured PDMS replicas were peeled, punched for holes for connection, oxidized, and then sealed to pre-cleaned and oxidized glass slides. The whole device was baked for another 10 min at 80°C to ensure strong bonding between PDMS and the glass slide. Platinum wires were inserted into the reservoirs (through PDMS wall at the inlet reservoir) and used as electrodes.

Reagents and Cell Culture

Chinese hamster ovary (CHO-K1) cells were incubated at 37°C , under 5% CO_2 in the Dulbecco's modified Eagle's medium (DMEM, Mediatech, Inc., Herndon, VA) supplemented with 10% (v/v) fetal bovine serum (FBS, Sigma, St. Louis, MO), penicillin (100 U/mL, Sigma), and streptomycin (100 $\mu\text{g}/\text{mL}$, Sigma). To maintain cells in the exponential growth phase ($\sim 1 \times 10^6$ cells/mL), they were diluted at a ratio of 1:5–1:8 every 2 days. The harvested cells were centrifuged at 300g for 10 min to remove the supernatant. Electroporation buffer (8 mM Na_2HPO_4 , 2 mM KH_2PO_4 , and 250 mM sucrose, $\text{pH} = 7.4$) was used to suspend the cell pallet for the subsequent delivery experiments. To prevent clogging, the electroporation buffer was filtered by a 0.2 μm filter.

Plasmid Preparation

The plasmid vector pEGFP-C1 (Clontech, Palo Alto, CA) was propagated in *Escherichia coli* and then extracted and purified using the Hispeed Plasmid Max Kit (Qiagen,

Valencia, CA). The plasmid was then dissolved in Tris-EDTA buffer and stored at -20°C until use.

Microchip Operation

Prior to the experiments, the channels were flushed with the electroporation buffer for 15 min to remove impurities. The inlet end of the channel was connected to a syringe pump (PHD infusion pump, Harvard Apparatus) through plastic tubing and the electrode (a Pt wire) on the inlet side was inserted into the reservoir through a hole in PDMS poked by a needle with a diameter slightly smaller than that of the Pt wire (as shown in Fig. 2). Flow rates ranging from 10 to $740\ \mu\text{L}/\text{min}$ were used in the experiments to control the cell velocity. We did not observe gas formation and cell clogging during our experiments owing to the fact the fluid was constantly flowing.

SYTOX[®] Green Delivery

Cells were suspended in the electroporation buffer with a concentration of 2×10^6 cells/mL. Two separate sets of tests were done. In one set of tests, SYTOX[®] green nucleic acid stain (MW ~ 600 , 504/523 nm, Invitrogen, Carlsbad, CA) was added to the cell sample in the electroporation buffer to

create a final concentration of $1\ \mu\text{M}$ before the electroporation. In the other set of tests, the cell sample was delivered into the device and electroporated first. Then SYTOX[®] green was added to the cell sample 1 h after the electroporation to achieve the same final concentration ($1\ \mu\text{M}$). The cells were collected from the receiving reservoir and transferred to a 96 well plate immediately after electroporation. To facilitate the observation, the 96 well plate was centrifuged at $300g$ for 10 min to settle the cells on the bottom. The images of cells were taken 1.5 h after the electroporation to obtain the percentages of fluorescent cells among the total population. Both phase contrast and fluorescent images of cells were taken at ten different locations in each sample. The area of each location was about $0.16\ \text{mm}^2$. These images were then analyzed to obtain the numbers for fluorescent and non-fluorescent cells with a total population of 2,000–3,000 being analyzed in each run. Every data point was based on three runs.

Due to the tiny amount of the cell sample generated by the microchip, techniques such as flow cytometry are not practical in here for examining the delivery.

Transfection With pEGFP-C1

The harvested cell pellet was re-suspended in the electroporation buffer containing $40\ \mu\text{g}/\text{mL}$ (unless otherwise described in the text) of pEGFP-C1 plasmid and then incubated on ice for at least 5 min before the electroporation. The final concentration of cells was $\sim 2 \times 10^6$ cells/mL. The mixture of cells and plasmid DNA was then dispensed into the device for electroporation. In each run, we infused a fixed volume ($\sim 40\ \mu\text{L}$) of cell suspension through the device to achieve about the same number of cells in the starting population of each sample. Immediately after electroporation, the sample was collected from the receiving reservoir and then transferred to a 96 well plate which contained fresh DMEM medium. The cells were then incubated at 37°C for 24 h and the viable cells would attach to the bottom the well plate. The sample was rinsed with phosphate buffer saline to remove dead cells and debris and then the number of cells attached to the bottom was compared to the control (at $0\ \text{V}/\text{cm}$) to determine the percentile viability. Phase contrast pictures were taken at ten different locations and the total number of attached cells in these areas was counted. The cell viability of the control (at $0\ \text{V}/\text{cm}$) experiment was considered as 100%. After the observation, the phosphate buffer saline was removed and replaced with fresh DMEM medium. The cells were then incubated for another 24 h before both the fluorescent cell number and the total cell number were enumerated to calculate the transfection frequency. Both phase contrast and fluorescent images of cells were taken at ten different locations in each sample. The area of each location was about $0.16\ \text{mm}^2$. A population of 2,000–3,000 cells was analyzed in each run. Every data point was based on three runs.

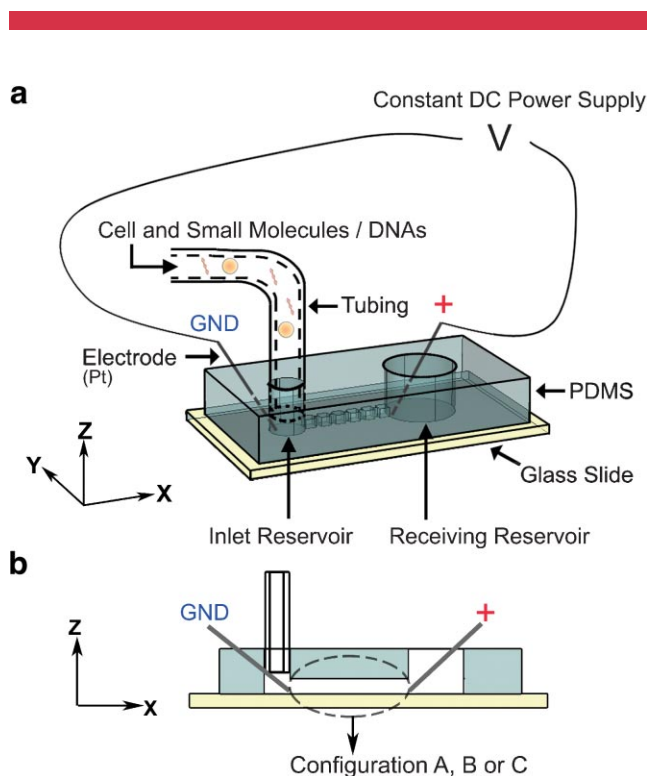


Figure 2. a: The setup of the microfluidic electroporation device. The device shown in the drawing is a configuration B device. b: The side view of the setup. The drawings are not to scale. [Color figure can be seen in the online version of this article, available at www.interscience.wiley.com.]

Phase Contrast and Fluorescence Microscopy

The cells were observed on an inverted fluorescence microscope (IX-71, Olympus, Melville, NY) with a 20X dry objective. The epifluorescence excitation was provided by a 100 W mercury lamp, together with brightfield illumination. The excitation and emission from cells loaded with SYTOX[®] Green or transfected with the plasmid were filtered by a fluorescence filter cube (Exciter HQ480/40, emitter HQ535/50, and beamsplitter Q505lp, Chroma Technology, Rockingham, VT). The images of the cells were taken with a CCD camera (ORCA-285, Hamamatsu, Bridgewater, NJ).

Results and Discussion

Design of the Device and Modeling of the Field Intensity Distribution

Figure 1a shows one part of the fabricated channel with the width reduction connecting a wide section with a narrow section. As shown in Figure 1b, devices with different designs (configurations A, B, and C) were applied in this study. The modeling of the field strength in the devices when a constant voltage across the channel is established suggests that the field strength in the narrow section is around eightfold higher than that in the bulk of the wide sections, regardless of the lengths associated with the sections (Fig. 1b). This agrees with the prediction from the Ohm' law that the field strength in each section is inversely proportional to the width in the section, when the depth of the channel is uniform. Table I summarizes the voltages applied in our experiments to a configuration A or B device and the resulted field intensities in different sections of the device. In our experiments (setup shown in Fig. 2), CHO-K1 in a buffer, which contained impermeant small molecules or plasmid DNA, flowed through the channel when a constant DC voltage was applied across the channel. Cells experienced pulse-like electric field variation(s) while flowing through the channel with alternating wide and narrow sections. We tested devices with a variety of layouts (configurations A, B, and C in Fig. 1b) which were analogous to the application of single or multiple pulses with different pulse patterns. The devices were fabricated based on PDMS using standard soft-lithography (Duffy et al., 1998).

The residence time is defined as the duration for cells to stay in a certain section of the channel and it was determined by the cell velocity and the length of the section. The velocity

Table I. The applied voltages across the device (V) and resulted field intensities in different sections (E_1 and E_2) of a configuration A or B device.

V (V)	41	55	69	83	96	110
E_1 (V/cm)	37	50	62	75	87	100
E_2 (V/cm)	300	400	500	600	700	800

E_1 and E_2 refer to the field intensities in the wide and narrow sections, respectively.

of the cells was controlled by a syringe pump which was connected to the inlet end of the device. We measured the cell velocity by tracking the movement of calcein AM (a fluorogenic dye) loaded cells under the microscope and found that the electric field had little contribution to the cell velocity (data not shown) at high flow rates applied in these experiments. The residence time of cells in the experiments was calculated based on the infusion rate of the syringe pump and the dimensions of the section. The contribution to the carrier flow velocity from electroosmotic flow (EOF) is minor compared to that from pressure-driven flow generated by the syringe pump. EOF velocity is estimated to be lower than 0.14 cm/s [at 800 V/cm with a mobility of 1.8×10^{-4} cm²/Vs from the literature (Wang W et al., 2006)], compared to 5–400 cm/s generated by the syringe pump. When desired, we were able to achieve the same total residence time in the narrow section(s) in devices of different configurations (A, B, and C) by having the total length of narrow sections and the infusion rates identical.

The current was stable during electroporation experiments and ranged from 0.01 to 0.06 mA (with 300–800 V/cm in the narrow section, respectively) in either configuration A or B devices. The Joule heating (or Ohmic heating) can be estimated based on the current and the voltage. In the worst case (with the lowest flow rate of 10 μ L/min, the highest voltage 110 V, and the highest current of 0.06 mA), the Joule heating roughly introduces ~ 9.4 K increase in the temperature of the solution, assuming no dissipation of the heat. The actual change in the solution temperature will be lower than this due to the dissipation of the heat through microchannel walls.

Delivery of a Membrane-Impermeant Dye SYTOX[®] Green

Our previous study indicated that the electric field inside the wide sections did not contribute to cell electroporation or death when the field intensity in there was substantially lower than the electroporation threshold (around 400 V/cm for CHO cells when the residence time was less than 100 ms in the narrow section) (Wang and Lu, 2006). Therefore, we focused on the effects of the residence time and field intensity in the narrow section(s) in most of this study.

In order to examine the ability of our device to deliver small molecules into CHO cells, we tested the delivery of SYTOX[®] Green, which was a nucleic acid stain impermeant to live cells and became fluorescent upon binding to DNA. We used the microfluidic device with one single narrow section (configuration A in Fig. 1b). Two sets of tests were performed to obtain the percentage of cells which were electropermeabilized and delivered with the molecule. First, SYTOX[®] Green was added to the cell suspension before electroporation. The cells were then processed by the microfluidic electroporation device under varying electrical parameters (field intensity and residence time in the narrow section) and the fluorescent and non-fluorescent cells were

enumerated. While in the second experiment, SYTOX[®] green was added 1 h after electroporation. In the first set of data (Fig. 3a), the percentage of fluorescent cells includes both the dead cells from the procedure and the live cells which were electroporatively delivered with the molecule,

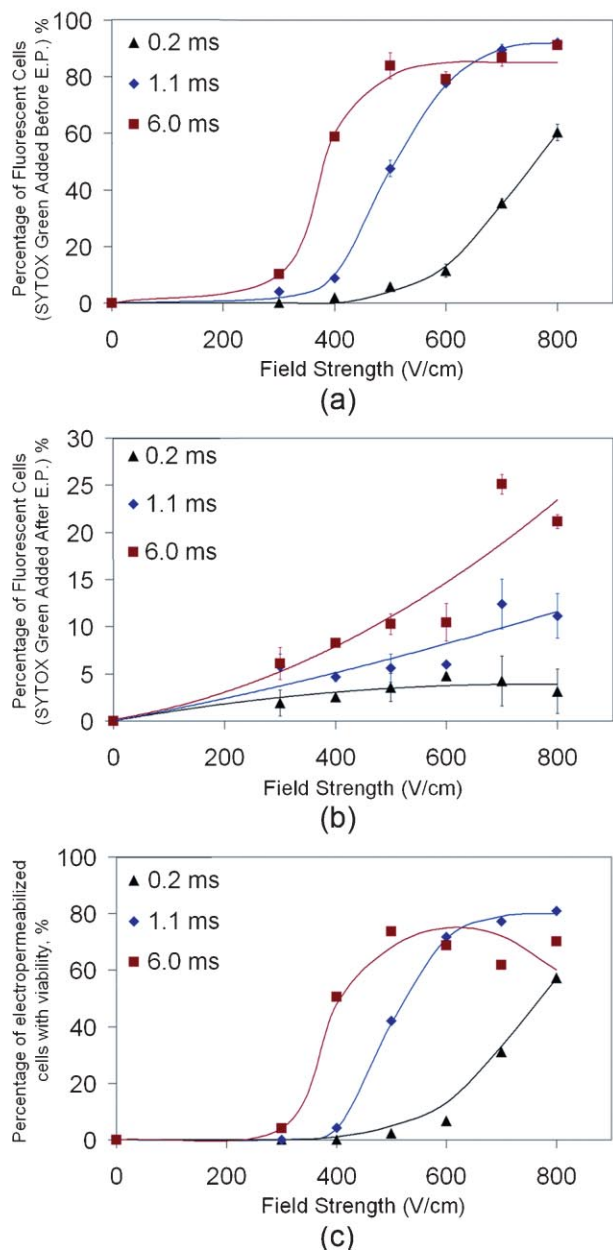


Figure 3. The delivery of SYTOX[®] Green into CHO-K1 cells. The experiment was carried out using configuration A devices. **a:** The percentage of fluorescent cells among the examined cell population after electroporation with varying field intensities and residence times in the narrow section when SYTOX[®] green was added to the cell sample before electroporation. **b:** The percentage of fluorescent cells after electroporation with varying field intensities and residence times in the narrow section when SYTOX[®] green was added to the cell sample 1 h after electroporation. **c:** The difference in the percentage between (a) and (b). This percentage represents the cells which were electroporated and remained viable after the delivery. [Color figure can be seen in the online version of this article, available at www.interscience.wiley.com.]

because the cell membrane got compromised in both cases. On the other hand, the second set of data (Fig. 3b) reflects only the cell death due to electroporation because it is known that the cell membrane reseals within minutes after electroporation in case that the viability of the cell is preserved (Prausnitz et al., 1995; Zimmermann et al., 1974). The difference between the two sets of data (Fig. 3c) indicates the fraction of the cells which were electroporatively delivered with the molecule and remained viable afterwards. As shown in Figure 3c, the percentage of electroporated cells with viability increased while the field intensity and the residence time in the narrow section increased up to the field intensity of 500–600 V/cm. When the field intensity increased further, the residence time of 6.0 ms appeared to be excessively long and this led to decrease in the percentage due to high rate of cell death. The percentage of cells delivered with the molecule while remaining viable could be as high as 80% when the electrical parameters were well tuned. The flow-induced shear stress did not seem to decrease cell viability significantly. The cell viability of the control (infused into the device when field strength was 0 V/cm) at all flow rates was similar to that of cells placed in the same electroporation buffer without running through the device. The size of CHO-K1 cells ranged from 10 to 16 μm before electroporation (Wang and Lu, 2006).

Transfection Using a Plasmid Vector Coding Green Fluorescent Protein

We also demonstrate the transfection of CHO cells with a plasmid vector. The pEGFP-C1 plasmid (4.7 kb, coding enhanced green fluorescent protein) was chosen to facilitate the observation of the delivery. In this part of the study, we tested devices with both configurations A and B (in Fig. 1b). The plasmid vector was added to the cell suspension and then the cell sample was processed by the microfluidic electroporation device under varying electrical parameters. We examined the cell viability after 24 h and the transfection after 48 h. Figure 4a–c shows a typical set of images (phase contrast, fluorescent, and overlay images) 48 h after cells were electroporatively delivered with the plasmid vector. A percentage of the cells expressed green fluorescent protein. Figure 4d and e shows the transfection frequency (the percentage of cells expressing EGFP among viable cells) with varying field intensities and residence times in the narrow section(s) of configuration A and B devices, respectively. In general, the transfection frequency increased when the field intensity in the narrow section(s) increased. However, longer residence times in the narrow section(s) did not always improve the transfection frequency. In Figure 4d, the increase from 1×0.2 to 1×1.1 ms introduced a rather large gain in the transfection frequency. However, further increase to 1×6.0 and 1×20 ms decreased the transfection frequency. Similar observation was made using configuration B devices (Fig. 4e). Such decrease in the transfection

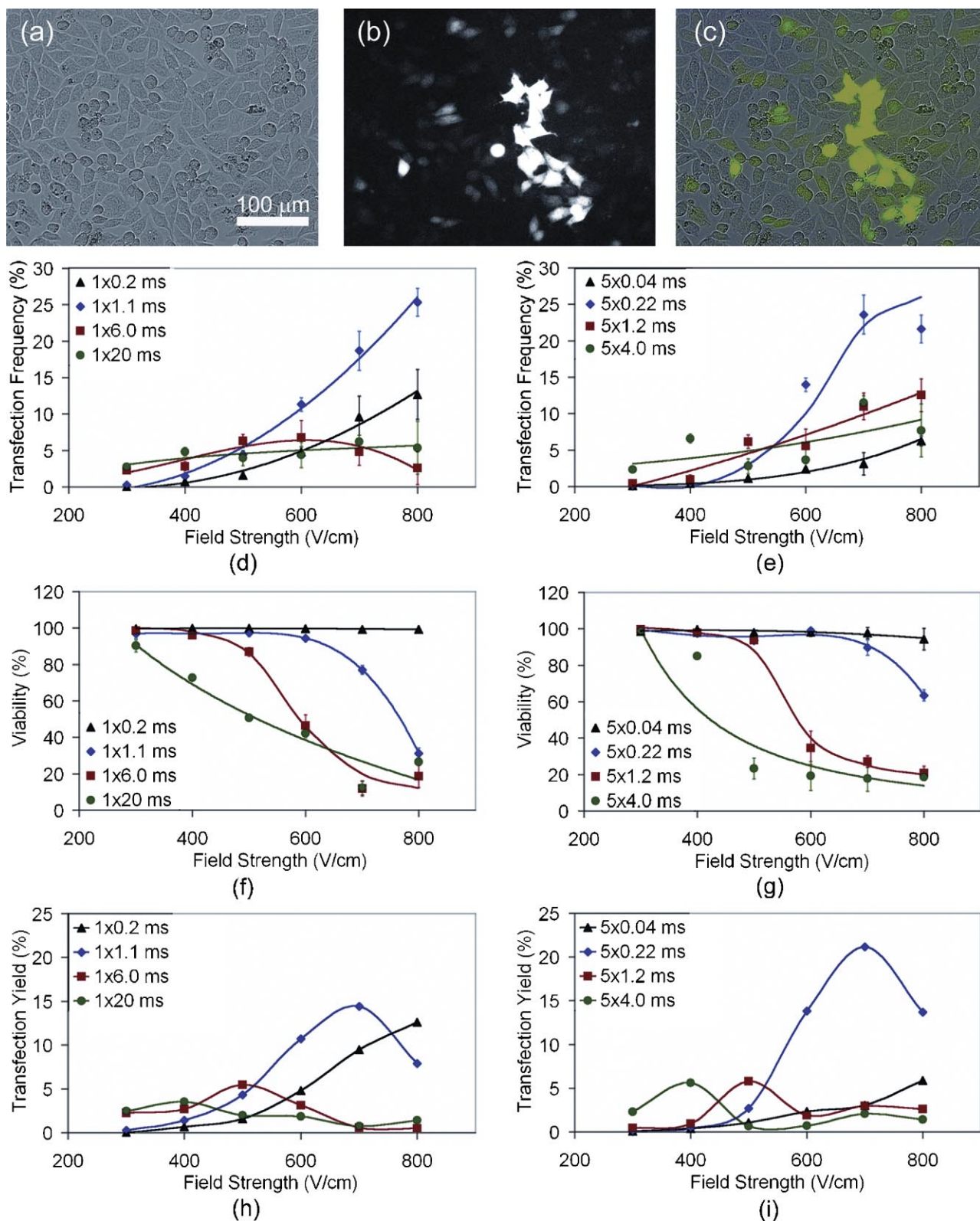


Figure 4. The transfection of CHO-K1 cells with the plasmid vector pEGFP-C1. **a:** The phase contrast image. **b:** The fluorescent image. **c:** The overlay image of (a) and (b). These cells were electroporated in a configuration A device with the residence time and field strength of 1.1 ms and 800 V/cm in the narrow section. The images were taken 48 h after electroporation. **d,e:** The transfection frequency (the percentage of cells expressing EGFP among viable cells) with varying field intensities and residence times in the narrow section(s) in configuration A and B devices, respectively. **f,g:** The percentage of viable cells in the starting cell population in configuration A and B devices, respectively. **h,i:** The transfection yield (the percentage of cells expressing EGFP in the starting cell population) in configuration A and B devices, respectively. The legends in (d) to (i) indicate the number of narrow section(s) and the residence time of cells inside each narrow section (e.g., 5×1.2 ms means that the device has five narrow sections and the residence time in each is 1.2 ms). [Color figure can be seen in the online version of this article, available at www.interscience.wiley.com.]

frequency at the longer residence times may indicate certain damage to cell functions due to Joule heating or the compromise of the membrane which leads to impaired capacity for gene expression. When the total residence time in the narrow section(s) was the same, devices of the two configurations yielded very comparable results in the transfection frequency. Figure 4f and g shows the percentage of viable cells after the gene delivery among the starting cell population. It is fairly consistent that the cell viability decreased with longer residence time and higher field intensity in the narrow section(s). Configuration B devices yielded better viability compared to that of configuration A devices especially with the total resident time at 1.1 and 6.0 ms. It needs to be noted that the viability estimated here is conservative because only the cells that attached to the substrate 24 h after electroporation were counted as viable. Figure 4h and i shows how the transfection yield (the product of transfection frequency and cell viability) varied with the electrical parameters. The transfection yield was defined as the percentage of cells expressing EGFP among the cells in the starting sample. The transfection yields with the residence times of 1×0.2 ms (Fig. 4h) and 5×0.04 ms (Fig. 4i) reached their maximum at the highest field intensity (800 V/cm). With the other longer residence time, the transfection yield reached its peak in between 400 and 700 V/cm, due to high loss in the viability at the higher field intensities. The data suggest that configuration B devices with multiple narrow sections offer a substantially higher optimum transfection yield (21.2% with 700 V/cm and 5×0.22 ms) than that of configuration A devices with single narrow section (14.4% with 700 V/cm and 1.1 ms). Compared to configuration A devices, this higher optimum transfection yield in configuration B devices was mostly contributed by the lower cell death when a medium total residence time was used.

Our data also suggest that the low electrical field in the wide sections may have considerable effects on the efficiency of gene delivery. In Figure 5, we examined the delivery of the plasmid DNA in configurations B and C devices (Fig. 1b). With the wide sections having the same dimensions in these two configurations, configuration B has narrow sections with half of the length as that of those in configuration C. In both configurations, we had 500 V/cm in the narrow sections and 62 V/cm in the wide sections for electroporative delivery. When we kept the total residence time in the narrow sections the same in these two configurations (5×0.22 ms), we had the residence time in the wide sections of configuration B (6×4.4 ms) two times longer than those in the configuration C (6×2.2 ms). Figure 5 shows that the transfection frequency was substantially higher in configuration B than that yielded by configuration C. This indicated that the low field in the wide sections could possibly enhance the delivery of DNA molecules when combined with the high field in the narrow sections. It has been suggested that low field with the intensity less than the electroporation threshold could improve the delivery efficacy by electrophoretically transporting DNA molecules

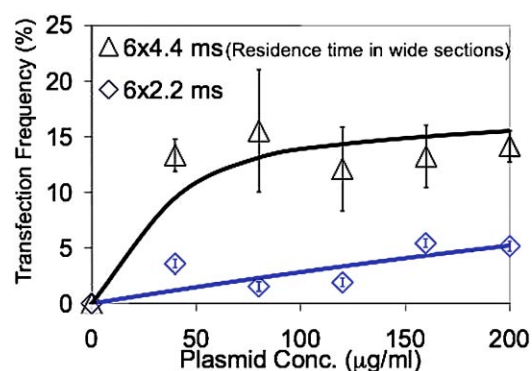


Figure 5. The effects of the residence times in the wide sections on the transfection frequencies. Configuration B and C devices were applied in the experiment. The residence times in the narrow sections were 5×0.22 ms in both configurations. The residence times in the wide sections were 6×4.4 ms in the configuration B and 6×2.2 ms in the configuration C. [Color figure can be seen in the online version of this article, available at www.interscience.wiley.com.]

deep into the cells (Bureau et al., 2000; Satkauskas et al., 2002, 2005). Our approach allows easy realization of such combination of high and low intensity fields by simply adjusting the geometry of the microfluidic device.

We also observed increased cell death at high plasmid concentrations. Figure 6 indicates that the transfection frequency did not vary significantly when the plasmid concentration was in between 40 and 200 µg/mL. However, the cell viability continued to drop when the plasmid concentration increased beyond 40 µg/mL. Similar phenomenon was observed during gene delivery based on electropulsation (Stacey et al., 1993).

Conclusions

In this study, we demonstrate delivery of impermeant small molecules and plasmid vectors into mammalian cells under

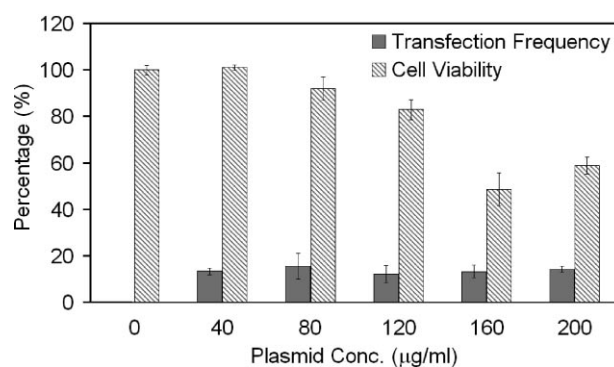


Figure 6. The toxicity of the plasmid vector to cells at high concentrations. Configuration B devices were used in this experiment. The total residence time inside five narrow sections was 6 ms (i.e., 5×1.2 ms). The field strengths inside the narrow and wide section were 500 and 62 V/cm, respectively.

constant DC voltage in a simple microfluidic device. Taking advantage of the transporting capability of microfluidics, we create field variation very similar to that of electric pulses when cells flow through the device. Since the field intensity change experienced by cells is essentially the same as that with conventional electropulsation, our technique has the potential to achieve delivery efficiency comparable to that of conventional electropulsation. Our results indicate that the devices with multiple narrow sections (equivalent of applying multiple pulses) can yield significantly better results in the final transfection yield than the devices with single narrow section (equivalent of applying single pulse), when the electrical parameters (the residence time and the field intensity in the narrow sections) are well tuned in both cases. The residence time in the wide sections also has significant impact on the transfection efficiency. These data suggest that our technique may offer some unique opportunities to improve delivery efficiency by optimizing the geometry of the device. As we described in previous reports and this study (Wang and Lu, 2006), the mechanism for electroporation to occur is not related to absolute dimensions of the fluidic structure. In principle, as long as the ratio in the cross-sectional area between different sections is kept, the device can be scaled up and down as desired. This potentially allows the processing of cell samples with volumes from milliliters to single cells based on the same principle. The application of constant voltage in our technique will allow simple and affordable instrumentation for electroporative delivery and easy integration with other analytical tools such as electrophoresis. Taking advantage of the small footprint, our technique and device will be ideal for high-throughput screening of genes/drugs by having a number of such devices working in parallel on the same chip.

This research was supported by Wallace H. Coulter Foundation through an Early Career Award to CL. The authors thank Dr. Zhao-Qing Luo at Biological Sciences of Purdue University for helpful discussions.

References

- Bureau MF, Gehl J, Deleuze V, Mir LM, Scherman D. 2000. Importance of association between permeabilization and electrophoretic forces for intramuscular DNA electrotransfer. *Biochim Biophys Acta* 1474:353–359.
- Duffy DC, McDonald JC, Schueller OJA, Whitesides GM. 1998. Rapid prototyping of microfluidic systems in poly(dimethylsiloxane). *Anal Chem* 70:4974–4984.
- Huang Y, Rubinsky B. 2003. Flow-through micro-electroporation chip for high efficiency single-cell genetic manipulation. *Sens Actuators A* 104:205–212.
- Khine M, Lau A, Ionescu-Zanetti C, Seo J, Lee LP. 2005. A single cell electroporation chip. *Lab Chip* 5:38–43.
- Lee SW, Tai YC. 1999. A micro cell lysis device. *Sens Actuators A* 73:74–79.
- Lin YC, Huang MY. 2001. Electroporation microchips for in vitro gene transfection. *J Micromech Microeng* 11:542–547.
- Lu H, Schmidt MA, Jensen KF. 2005. A microfluidic electroporation device for cell lysis. *Lab Chip* 5:23–29.
- Munce NR, Li J, Herman PR, Lilge L. 2004. Microfabricated system for parallel single-cell capillary electrophoresis. *Anal Chem* 76:4983–4989.
- Neumann E, Schaefer-Ridder M, Wand Y, Hofschneider P. 1982. Gene transfer into mouse lymphoma cells by electroporation in high electric fields. *EMBO J* 1:841–845.
- Okino M, Mohri H. 1987. Effects of a high-voltage electrical impulse and an anticancer drug on in vivo growing tumors. *Jpn J Cancer Res* 78: 1319–1321.
- Pavlin M, Kanduser M, Rebersek M, Pucihar G, Hart F, Magjarevic R, Miklavcic D. 2005. Effect of cell electroporation on the conductivity of a cell suspension. *Biophys J* 88:4378–4390.
- Prausnitz MR, Corbett JD, Gimm JA, Golan DE, Langer R, Weaver JC. 1995. Millisecond measurement of transport during and after an electroporation pulse. *Biophys J* 68:1864–1870.
- Satkauskas S, Bureau MF, Puc M, Mahfoudi A, Scherman D, Miklavcic D, Mir LM. 2002. Mechanisms of in vivo DNA electrotransfer: Respective contributions of cell electroporeabilization and DNA electrophoresis. *Mol Ther* 5:133–140.
- Satkauskas S, Andre F, Bureau MF, Scherman D, Miklavcic D, Mir LM. 2005. Electrophoretic component of electric pulses determines the efficacy of in vivo DNA electrotransfer. *Hum Gene Ther* 16:1194–1201.
- Stacey K, Ross I, Hume D. 1993. Electroporation and DNA-dependent cell death in murine macrophages. *Immunol Cell Biol* 71:75–85.
- Wang HY, Lu C. 2006. Electroporation of mammalian cells in a microfluidic channel with geometric variation. *Anal Chem* 78:5158–5164.
- Wang HY, Bhunia AK, Lu C. 2006. A microfluidic flow-through device for high throughput electrical lysis of bacterial cells based on continuous dc voltage. *Biosens Bioelectron* 22:582–588.
- Wang W, Zhao L, Jiang LP, Zhang JR, Zhu JJ, Chen HY. 2006. EOF measurement by detection of a sampling zone with end-channel amperometry in microchip CE. *Electrophoresis* 27:5132–5137.
- Zimmermann U, Pilwat G, Riemann F. 1974. Dielectric-breakdown of cell membranes. *Biophys J* 14:881–899.